The Journal of Chemical Physics

The vapor pressure of liquid and solid water phases at conditions relevant to the atmosphere

Cite as: J. Chem. Phys. **151**, 064504 (2019); https://doi.org/10.1063/1.5100364
Submitted: 17 April 2019 . Accepted: 18 July 2019 . Published Online: 09 August 2019

Mario Nachbar, Denis Duft, and Thomas Leisner

The Journal of Chemical Physics ARTICLE scitation.org/journal/jcp

The vapor pressure of liquid and solid water phases at conditions relevant to the atmosphere

Cite as: J. Chem. Phys. 151, 064504 (2019); doi: 10.1063/1.5100364
Submitted: 17 April 2019 • Accepted: 18 July 2019 •
Published Online: 9 August 2019

Mario Nachbar,[1] Denis Duft,[1] and Thomas Leisner[1,2,a)]

AFFILIATIONS

[1]Institute for Meteorology and Climate Research, Karlsruhe Institute of Technology, P.O. Box 2640, Karlsruhe, Germany
[2]Institute of Environmental Physics, Heidelberg University, Im Neuenheimer Feld 229, D-69120 Heidelberg, Germany

Note: This paper is part of a JCP Special Topic on Chemical Physics of Supercooled Water.
[a)]**Author to whom correspondence should be addressed:** Thomas.Leisner@kit.edu

ABSTRACT

In the atmosphere, water can be present in liquid and solid phases, but the vapor phase is generally predominant. Condensed phases of water occur under a wide range of conditions, ranging from polar mesospheric clouds at the lowest atmospheric temperatures and at low pressure to the much warmer tropospheric clouds. The temperature range at which ice or water clouds are observed spans from T = 100 to 300 K with pressures ranging from about 10^{-3} mbar to about 1 bar. Over this wide range, water is known to form several condensed phases, which can be separated into crystalline (hexagonal and stacking disordered ice) and noncrystalline phases (liquid and supercooled liquid water, amorphous solid water). We report on the vapor pressure of these water phases with a focus on metastable amorphous solid water and stacking disordered ice in the light of recent experimental findings and discuss possible implications for the atmosphere. We present evidence that supercooled liquid water and low density amorphous solid water do not belong to the same phase and therefore, no continuous vapor pressure curve can be given.

INTRODUCTION

The formation of condensed phases of water (clouds) in the atmosphere is of prime importance for the global heat and water budget. Liquid and ice clouds interact both with the incoming solar and with the outgoing thermal radiation, and their formation and dissolution is accompanied by a considerable transfer between latent and sensible heat. In order to describe these processes reliably, the thermodynamic properties and especially the vapor pressures of the condensed phases involved need to be known. Atmospheric cloud formation occurs under a wide range of conditions, from polar mesospheric clouds, which form at the lowest atmospheric temperatures and at low pressure,[1–3] to the much warmer tropospheric clouds. The temperature range at which ice or water clouds are observed spans from T = 100 to 300 K with pressures ranging from about 10^{-3} mbar to about 1 bar. Over this wide range, water is known to form several condensed phases, which can be separated into crystalline (hexagonal and stacking disordered or cubic ice) and noncrystalline phases (liquid and supercooled liquid water, amorphous solid water).

Liquid water is the stable condensate of water at temperatures above the triple point. Below the triple point, liquid water is metastable and crystallizes into the stable hexagonal ice I_h. Liquid water may be supercooled to about 235 K before crystallization sets in on atmospheric time scales.[4] This water phase is then referred to as supercooled liquid water (SLW).

When water vapor condenses below about 160 K,[5–10] it forms a noncrystalline solid form of water, so called amorphous solid water (ASW). Depending on the production pathway, different ASW polymorphs exist.[11] The ASW polymorph which forms from the vapor phase under atmospheric conditions is called low density amorphous solid water, which we will refer to as ASW in the following. ASW has been proposed to be the low temperature form of SLW,[12–15] but this assertion is still controversially discussed.[11,16] ASW is metastable and converts to crystalline ice on atmospheric time scales at a temperature above about 130 K.

The crystalline ice phase that forms in the crystallization process of ASW was originally referred to as cubic ice.[17] Recent

studies based on numerical simulations[18–27] and diffraction measurements[23,28–31] found, however, that pure cubic ice is difficult to obtain and that ice samples which had been labeled cubic ice were actually sequences of cubic ice interlaced with sequences of hexagonal ice. This crystalline ice polymorph was termed stacking disordered ice I_{sd}. Ice I_{sd} is metastable and transforms to ice I_h above about 200 K with a transformation time depending on temperature[28,32] and particle size.[32]

Under atmospheric conditions, crystalline ice may not only form upon heating of ASW but can also be deposited directly from the vapor phase at temperatures above 160 K. Experimental studies indicate that deposition temperatures above 200 K result in the formation of ice I_h[33–37] and deposition temperatures below 200 K are likely to cause the formation of ice I_{sd}.[33,37]

High precision direct vapor pressure measurements are available for crystalline ice[38–45] down to about 170 K but for liquid water[46–49] only down to temperatures of about 260 K. These data combined with the measurements of the heat capacity of ice I_h[50,51] and SLW[52–54] (T > 236 K) allowed the parameterization of the water vapor pressures of ice I_h[55–57] (T > 100 K) and SLW[55] (T > 235 K) with an accuracy better than 1%. The vapor pressures of the metastable solid phases ice I_{sd} and ASW on the contrary are much more uncertain, as they can be studied for reasonably long time scales only at temperatures below 200 K for ice I_{sd} and below 150 K for ASW. The extremely low vapor pressures at these temperatures (on the order of 10^{-10} mbar at 130 K) render direct vapor pressure measurements unfeasible. However, a number of studies were performed employing quartz crystal microbalances[58,59] or quadrupole mass spectrometers[15,59–65] to measure the sublimation rates of ASW and of ice I_{sd} samples crystallized from ASW. It is possible to infer the vapor pressure from sublimation rate data under the well supported assumption that the sticking coefficient of water molecules on water ice is unity at these temperatures.[62,66–71] However, such experiments are still very challenging (sublimation rates are about one monolayer per hour at 130 K) which is why the saturation vapor pressures inferred from sublimation rate data typically exhibit high uncertainties and the results vary by more than an order of magnitude.

An alternative approach for deducing the vapor pressure of ice I_{sd} and ASW exploits the fact that metastable water phases have a higher vapor pressure ($p_{sat,m}$) than the stable hexagonal ice phase ($p_{sat,hex}$) which is reflected in a Gibbs free energy difference $\Delta G_{m\to h}$ of the metastable phase with respect to ice I_h according to

$$p_{sat,m} = p_{sat,hex} \cdot \exp\left(\frac{\Delta G_{m\to h}}{RT}\right), \tag{1}$$

where R is the ideal gas constant and T the temperature in Kelvin. $\Delta G_{m\to h}$ relates to the enthalpy difference $\Delta H_{m\to h}$ and the entropy difference $\Delta S_{m\to h}$ according to

$$\Delta G_{m\to h} = \Delta H_{m\to h} - T \cdot \Delta S_{m\to h}. \tag{2}$$

The enthalpy difference $\Delta H_{m\to h}$ can be determined from the heat release observed in differential scanning calorimetry (DSC) experiments during the warm up of ASW and ice I_{sd} samples. However, the available DSC data of $\Delta H_{m\to h}$ range between 1280 J mol^{-1} and 2600 J mol^{-1} for ASW[8,12,72–77] and between 20 J mol^{-1} and 180 J mol^{-1} for ice I_{sd}.[73,78–81] This translates into a vapor pressure uncertainty of about 300% for ASW and of about 15% for ice I_{sd}.

Recent experimental findings[5,6] in our laboratory now permit to constrain more accurately the vapor pressures of these metastable ice phases, thereby drawing a more consistent picture of the vapor pressure of all atmospherically relevant ice phases. In this contribution, we will focus on ice I_{sd} and ASW. For a thorough discussion of the vapor pressure of hexagonal ice and supercooled liquid water, we refer to the seminal work of Murphy and Koop.[55]

CRYSTALLINE ICE I_{sd}

Just as hexagonal ice I_h, cubic ice I_c consists of identical layers with a hexagonal symmetry with the exception of a difference in the stacking order of these layers. While in hexagonal ice the layering is in the sequence of ABAB, the layering in cubic ice is ABCABC.[22,28] Because of their structural similarity, it is generally assumed that the vapor pressures of cubic and hexagonal ice and hence also the vapor pressures of stacking disordered ice I_{sd} and hexagonal ice I_h do not differ very much. Indeed, experiments[82] and model studies[18,83–85] show that the Gibbs free energy difference between cubic and hexagonal ice $\Delta G_{c\to h}$ is smaller than 10 J mol^{-1}. According to Eq. (1), this corresponds to a vapor pressure of ice I_c at most 1.2% higher than that of ice I_h above 100 K. Consequently, the vapor pressure of ice I_{sd} is assumed to be similarly close to ice I_h in this temperature range.

Figure 1 summarizes high quality literature data on the vapor pressure of crystalline ice which was deposited at temperatures below 220 K and therefore might be considered to consist of ice I_{sd}. The data were normalized to the vapor pressure of ice I_h according to the parameterization of Murphy and Koop,[55]

$$p_{sat,h} = \exp\left(9.550\,426 - \frac{5723.265}{T} + 3.530\,68 \cdot \ln(T) - 0.007\,283\,32 \cdot T\right), \tag{3}$$

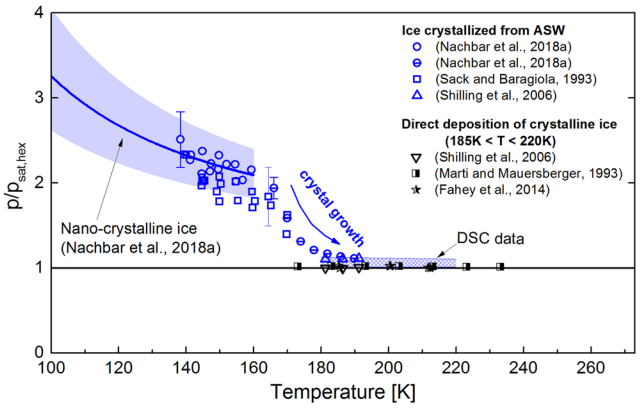

FIG. 1. Survey of vapor pressure measurements of crystalline ice phases deposited below 220 K. The blue data points (circles, squares, and triangles) represent ice crystallized from ASW and the black data points (squares, stars, and triangles) represent crystalline ice directly deposited from the vapor phase. The blue crosshatched pattern reflects the vapor pressure of ice crystallized from ASW deduced from the heat release observed in DSC measurements. The blue line represents the parameterization of nanocrystalline ice [Eqs. (4) and (1)] including a shaded interval of uncertainty.

with p in Pa and T in K. The experimental data presented in Fig. 1 deviate by up to a factor of 3 from the vapor pressure of stable hexagonal ice I_h. This discrepancy can be reconciled by separating the data in two data sets: (1) ice crystallized from ASW (blue data points) and (2) crystalline ice deposited directly from the vapor phase (black data points).

For the preparation of ice I_{sd} from ASW (group 1, blue data points in Fig. 1), ASW was created by vapor deposition at temperatures below 130 K and allowed to crystallize at temperatures above 130 K. It is well known that below 160 K the crystallization process of ASW proceeds via the formation of nanocrystals[86–90] which have been found to be stable for hours.[6,31] Recently, we showed[6] that the vapor pressure of such nanocrystalline ice is higher compared to bulk ice I_{sd} due to an increased surface to volume energy ratio (Kelvin effect). Interestingly, the size of the nanocrystals is independent of temperature below 160 K forming a seemingly stable polymorph (ice I_n) in this temperature range. Its vapor pressure $p_{sat,n}$ is parameterized on the basis of the reported crystal sizes ($d \approx 10$ nm)[88–92] and our vapor pressure measurements with a Gibbs free energy difference to ice I_h of[6]

$$\Delta G_{n\to h} = 982 \pm 182 \text{ J mol}^{-1}. \quad (4)$$

The corresponding saturation vapor pressure [Eq. (1)] of ice I_n is represented in Fig. 1 by the blue line including a shaded interval of uncertainty. Above 160 K, the crystal growth is thermally activated[6,31] thereby reducing the relative vapor pressure difference to hexagonal ice.

The vapor pressure of ice I_{sd} crystallized from ASW (group 1, blue data points in Fig. 1) levels off to a value about 10% higher than that of ice I_h. This 10% increase of the vapor pressure is in agreement with the results obtained from differential scanning calorimetry (DSC) experiments[78–81] observing a heat release ΔH between 20 J mol^{-1} and 180 J mol^{-1} while heating an ice sample crystallized from ASW in the temperature range of 180–220 K. Assuming that ΔS is close to zero,[93,94] this heat release corresponds to an elevation of the vapor pressure from 1% to 13% between 180 and 220 K which is represented by the blue crosshatched pattern in Fig. 1. On this basis, it was inferred that the vapor pressure of ice I_{sd} is about 10% higher than that of ice I_h.[35,55] This, however, is in conflict with the expected low Gibbs free energy difference of less than 10 J mol^{-1} between the two ice phases. Model studies[18] suggest that defects beyond stacking faults and pockets of unassociated water molecules are incorporated in the ice I_{sd} matrix during the crystallization process and might explain the observed high energy difference between the ice crystallized from ASW and ice I_h.

The black data points in Fig. 1 (group 2) show experimental data on the vapor pressure of crystalline ice phases which were deposited from the vapor phase at temperatures between 185 and 220 K. Shilling *et al.*[35] (black triangles) and Marti and Mauersberger[44] (black squares) deposited water vapor at temperatures above 200 K, where ice I_h forms, and measured the vapor pressure of the resulting deposits down to a temperature of 170 K. Fahey *et al.*[95] (black stars) performed expansion experiments in a cloud chamber and directly determined the gas phase vapor pressure in a thick ice cloud by optical absorption measurements. The data thus represent both the temperature of deposition and of measurement. They acquired data for temperatures down to 185 K for which the formation of ice I_{sd} is expected. All these data points do not deviate significantly from unity (hexagonal ice), which indicates that ice I_{sd} deposited from the vapor phase exhibits only a marginal degree of defects and supports the conclusion that the vapor pressure of defect free ice I_{sd} is very close to that of ice I_h.

AMORPHOUS SOLID WATER

ASW forms by the deposition of water vapor at temperatures below about 160 K.[5–10] It may assume a highly porous form,[96–104] with the degree of porosity depending on deposition temperature, deposition rate, and deposition angle with respect to the surface normal. Porous ASW exhibits a higher vapor pressure than compact ASW[61] and predominantly forms at temperatures below the range of atmospheric interest. ASW deposited between 90 and 110 K either resulted in nonporous ASW[97,102] or ASW with only a very small degree of porosity[8,62] and the ASW deposited above 110 K was shown to be compact.[96,102] The porosity of ASW produced at temperatures below 100 K strongly decreased during warm-up to temperatures above 100 K and resulted in compact ASW above 140 K.[97,100,101] Therefore, the ASW formed under atmospheric conditions (above 100 K) is predominantly compact ASW.

Recently, we reported novel vapor pressure measurements which show a surprisingly high vapor pressure of ASW.[5] The ASW samples were deposited under atmospherically relevant conditions in a process known to yield compact ASW.[5,7] However, since we do not have direct *in situ* evidence for the surface area of the ASW samples, we cannot exclude the possibility that they exhibit a small degree of porosity. These data are presented by the red circles in Fig. 2, where we also present literature vapor pressure data of ASW which were partially reanalyzed, as we will discuss below. Sack and Baragiola[59] deposited ASW onto a quartz crystal microbalance and performed isothermal sublimation rate measurements to observe the crystallization process of the ASW sample. They avoided the deposition of water molecules originating from external sources by shielding the sample with surfaces held at 12 K, thereby attaining high precision sublimation rate data. We took their ASW data, transferred the sublimation rates to vapor pressures and present them by the red squares in Fig. 2. Sublimation rates of ASW presented by other authors exhibit higher uncertainties.[15,60–64] The studies of Speedy *et al.*,[15] Smith *et al.*,[63] and Fraser *et al.*,[64] however, can be reanalyzed to obtain more accurate data. These authors used a quadrupole mass spectrometer to determine the sublimation rate of ASW samples during temperature ramping. After crystallizing the sample eventually below 160 K, the sample was cooled again and the sublimation of crystalline ice was measured under otherwise unchanged conditions. We assume that in fact nanocrystalline ice formed in these studies and that the relative vapor pressure difference between ASW and nanocrystalline ice obtained from these experiments are more precise than the absolute vapor pressure values. Therefore, we first normalized the raw data for ASW of Speedy *et al.*[15] and Smith *et al.*[63] to their results for crystalline ice and then multiplied the result with $\exp\left(\frac{982 \text{ J mol}^{-1}}{RT}\right)$, i.e., the parameterization of the vapor pressure of nanocrystalline ice. Similarly, we reanalyzed the data of Fraser and co-workers.[64] The results are presented by the brown, orange, and red-dashed lines in Fig. 2. They are in remarkably good agreement with our data as well as with the data of Sack and Baragiola.[59] However, they lie about a factor of three above the previously

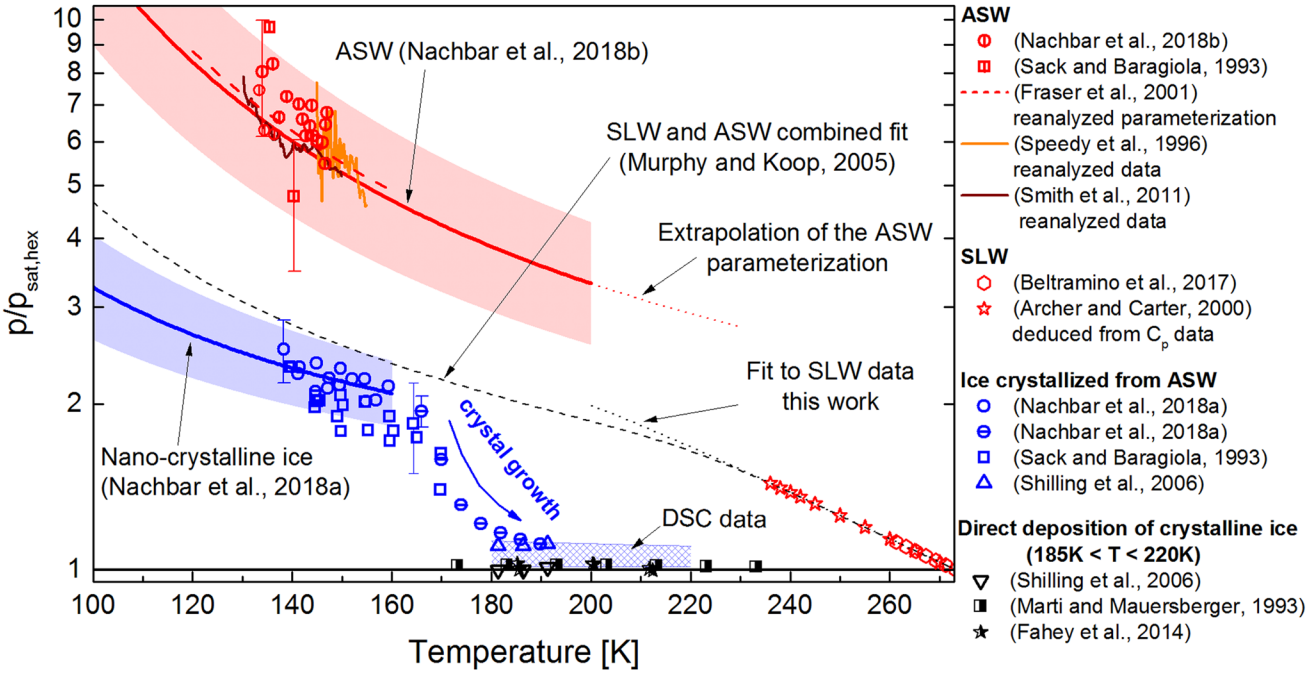

FIG. 2. Survey of vapor pressure measurements of atmospherically relevant water phases. The red dashed line, red squares, and circles as well as the brown and orange lines represent experimental data for ASW. The red stars and diamonds represent data for SLW deduced from heat capacity data and obtained via direct vapor pressure measurements, respectively. The blue and black data points represent crystalline ice, and are carried over from Fig. 1. The lines marked with arrows represent vapor pressure parameterizations discussed in the text, with the shaded areas indicating the interval of uncertainty.

assumed vapor pressure of ASW, which was constrained from measurements of the Gibbs free energy difference upon crystallization of ASW.[15,55]

In order to understand this discrepancy, we recently[5] reanalyzed all available DSC studies of ASW[8,12,72–77] under the assumption that ASW converts into nanocrystalline ice below 160 K and that the heat capacities of ASW and hexagonal ice show no significant difference between 60 and 200 K.[8,80,105] This analysis resulted in a consistent picture of the available $\Delta H_{a\to h}$ data and allowed us to derive an independent parameterization of the vapor pressure of ASW,

$$\Delta G_{a\to h} = (2312 \pm 227)\ \mathrm{J\ mol^{-1}} - T[K] \cdot (1.6 \pm 1)\ \mathrm{J\ mol^{-1}\ K^{-1}}, \tag{5a}$$

$$p_{sat,a} = p_{sat,hex} \cdot \exp\left(\frac{\Delta G_{a\to h}}{RT}\right). \tag{5b}$$

The corresponding saturation vapor pressure of ASW is represented in Fig. 2 by the red line including a shaded interval of uncertainty. It shows an almost perfect agreement with the vapor pressure data of ASW presented above. This agreement lends strong support for the existence and the properties of nanocrystalline ice as discussed in the section titled Crystalline Ice I_{sd}. Further DSC studies with varying heating rates are of desire in order to confirm this parameterization. Such studies should be able to observe and quantify the transition from well-annealed ASW to nanocrystalline or macrocrystalline ice depending on the heating rate and the crystallization temperature.

It is commonly assumed that compact ASW and SLW constitute the same thermodynamic phase.[55] This requires the existence of a continuous and non-negative function $\Delta c_p(T)$, representing the difference in the specific heat at constant pressure between the metastable phase and ice I_h. This function needs to connect the heat capacity data from the warmest known temperature of existence of ASW (T_c = 200 K) to the coldest known temperature of existence of SLW (T_w = 236 K). $\Delta c_p(T)$ is restrained by the following four boundary conditions:

$$\Delta c_p(T_c) \approx 0\ \mathrm{J\ mol^{-1}\ K^{-1}}, \tag{6a}$$

$$\Delta c_p(T_w) \approx 64\ \mathrm{J\ mol^{-1}\ K^{-1}}, \tag{6b}$$

$$\Delta H_{SLW\to h}(T_w) - \Delta H_{a\to h}(T_c) = \int_{T_c}^{T_w} \Delta c_p(T)\,dT \approx 2000\ \mathrm{J\ mol^{-1}}, \tag{6c}$$

$$\Delta S_{SLW\to h}(T_w) - \Delta S_{a\to h}(T_c) = \int_{T_c}^{T_w} \Delta c_p(T)\,d\ln T \approx 13.8\ \mathrm{J\ mol^{-1}\ K^{-1}}. \tag{6d}$$

The numerical values appearing above reflect the measured or newly derived differences in heat capacity,[8,53] enthalpy ΔH,[5,106] and entropy ΔS[5,63,106] between the involved phases and ice I_h.[55] It turns

out that no such function exists, i.e., whenever either three conditions are satisfied, the fourth boundary condition is violated even if $\Delta c_p(T)$ is taken to unphysical extremes. These findings hint that ASW and SLW may not be the same phase.

This would have important implications for atmospheric physics even at much warmer temperatures as ASW was assumed to belong to the same thermodynamic phase as SLW. The vapor pressure of ASW (as it was known then) was used by Murphy and Koop[55] to derive a unified vapor pressure curve that extends from SLW through the "no man's land" region to ASW (black dashed line in Fig. 2). This parameterization is frequently used in the atmospheric science community to calculate supersaturations with respect to liquid water. If however ASW and SLW are two distinct phases, this parameterization is called into question. We would rather recommend to fit the available experimental data of SLW and extrapolate to lower temperatures. In Fig. 2, we show the most recent data for the vapor pressure of SLW deduced from heat capacity data[53] and obtained via direct vapor pressure measurements[47] (red stars and diamonds, respectively) and a fit using the analytical form proposed by Murphy and Koop[55] (black dotted line) given by

$$p_{sat,SLW} = \exp\left(74.8727 - \frac{7167.405\,48}{T} - 7.771\,07 \cdot \ln(T) + 0.005\,05 \cdot T\right), \quad (7)$$

with p in Pa and T in K.

CONCLUSION

In summary, we present here a new and unifying view on the various phases which may be encountered in the atmosphere. These phases, their transformation temperatures, and respective vapor pressures are compiled in Fig. 3 together with the references they are based on. In order to provide further evidence for this new view, we call for DSC experiments which explicitly study the phase transitions from well-annealed ASW to nanocrystalline and macrocrystalline ice.

Condensation of water vapor in the atmosphere below about 160 K seems to proceed inevitably via compact ASW. The vapor pressure of ASW is higher than previously assumed[55] and can be parameterized with Eq. (5), which is valid below 200 K. ASW is metastable with respect to crystalline ice and crystallization times are strongly temperature dependent. They range from several days at 125 K to less than a minute at 160 K for compact ASW samples.[63,107–109] Thus, ASW may be encountered in the atmosphere at temperatures below about 160 K. In particular, we assume that ASW is the phase of ice condensing during the formation of noctilucent clouds in the mesopause.[7] Depending on the meteorological conditions, crystalline ice may eventually develop in these clouds. Similar conclusions can be drawn for water ice clouds on other planets like Mars, where they are frequently encountered at temperatures below 160 K.[110–112]

The crystallization process of ASW forms nanocrystals with a diameter of about 10 nm composed of stacking disordered ice I_{sd}. The nanocrystals exhibit a vapor pressure higher than that of bulk ice I_{sd}. They are stable for hours below 160 K such that nanocrystalline ice I_n may be regarded as a separate phase below 160 K. The vapor pressure for ice I_n is parameterized in Eq. (4).

Above 160 K, crystal growth is effectively activated in ice I_n which is accompanied by a reduction of the vapor pressure difference to bulk ice I_{sd}. This process is likely to leave defects and unassociated water molecules in the ice I_{sd} matrix, which results in a vapor pressure of this ice polymorph being about 10% higher than that of hexagonal ice I_h between 180 and 190 K. At even higher temperatures, these defects heal and the vapor pressure assumes that of ice I_{sd}, which is at most one percent higher than that of ice I_h.

Our findings imply that ASW and SLW are distinct phases of water and a phase transition may occur somewhere in the "no man's land" region between 200 K and 230 K. An unconstrained extrapolation of SLW data into the temperature range below 235 K yields higher values than the parameterization of Murphy and Koop.[55] This might help to understand water vapor concentration measurements in the tropical tropopause region that fall above the Murphy-Koop line.[113,114]

Water and its low temperature polymorphs remain full of surprises and more experimental and theoretical work is clearly needed. Especially, the hypothesized phase transition between SLW and ASW between 230 K and 200 K needs more attention. One straight way forward could be via studies of the condensation of gas phase water onto hydrophobic surfaces in this temperature range. They might reveal a transition from SLW to ASW as the first phase forming when lowering the temperature. This transition would be detectable as a discontinuity in the water vapor pressure at the condensation threshold.

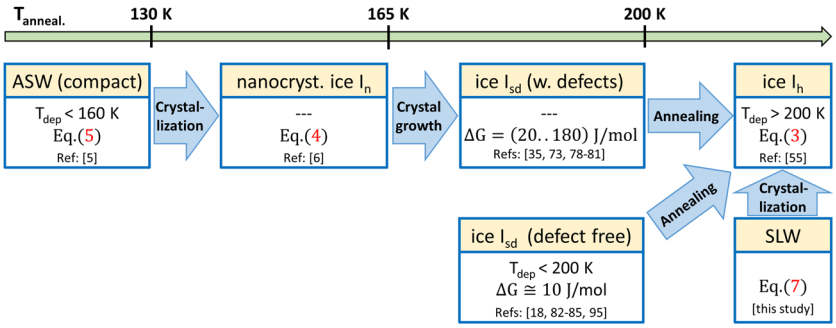

FIG. 3. Summary of the formation and transformation temperatures of the different water phases which may be encountered in the atmosphere. ΔG values are with respect to ice I_h. The references contain the data used to derive the ΔG values and the vapor pressure equations given in the manuscript.

ACKNOWLEDGMENTS

The authors thank Thomas Dresch and Thomas Koop for valuable discussions. This work was partially funded by the German Federal Ministry of Education and Research (BMBF, Grant No. 05K16VHB), the German Research Foundation (DFG, Grant No. LE 834/4-1), and the Helmholtz Association in the framework of the program Atmosphere and Climate.

REFERENCES

[1] M. Rapp and F. J. Lübken, Atmos. Chem. Phys. **4**, 2601 (2004).
[2] M. Rapp, F. J. Lübken, A. Müllemann, G. E. Thomas, and E. J. Jensen, J. Geophys. Res.: Atmos. **107**, 4392, https://doi.org/10.1029/2001JD001241 (2002).
[3] F. J. Lübken, J. Lautenbach, J. Höffner, M. Rapp, and M. Zecha, J. Atmos. Sol.-Terr. Phys. **71**, 453 (2009).
[4] H. R. Pruppacher and J. D. Klett, *Microphysics of Clouds and Precipitation*, 2nd ed. (Kluwer Academic Publishers, Dordrecht, 2004).
[5] M. Nachbar, D. Duft, and T. Leisner, J. Phys. Chem. B **122**, 10044 (2018).
[6] M. Nachbar, D. Duft, and T. Leisner, Atmos. Chem. Phys. **18**, 3419 (2018).
[7] D. Duft, M. Nachbar, and T. Leisner, Atmos. Chem. Phys. **19**, 2871 (2019).
[8] M. Chonde, M. Brindza, and V. Sadtchenko, J. Chem. Phys. **125**, 094501 (2006).
[9] S. Mitlin and K. T. Leung, J. Phys. Chem. B **106**, 6234 (2002).
[10] S. Mitlin and K. T. Leung, Can. J. Chem. **82**, 978 (2004).
[11] K. Amann-Winkel, R. Böhmer, F. Fujara, C. Gainaru, B. Geil, and T. Loerting, Rev. Mod. Phys. **88**, 011002 (2016).
[12] G. P. Johari, G. Fleissner, A. Hallbrucker, and E. Mayer, J. Phys. Chem. **98**, 4719 (1994).
[13] O. Mishima and H. E. Stanley, Nature **396**, 329 (1998).
[14] O. Mishima and H. E. Stanley, Nature **392**, 164 (1998).
[15] R. J. Speedy, P. G. Debenedetti, R. S. Smith, C. Huang, and B. D. Kay, J. Chem. Phys. **105**, 240 (1996).
[16] A. K. Soper, Nat. Mater. **13**, 671 (2014).
[17] P. V. Hobbs, *Ice Physics* (Oxford University Press, New York, 1974).
[18] A. Hudait, S. Qiu, L. Lupi, and V. Molinero, Phys. Chem. Chem. Phys. **18**, 9544 (2016).
[19] L. Lupi, A. Hudait, B. Peters, M. Grünwald, R. Gotchy Mullen, A. H. Nguyen, and V. Molinero, Nature **551**, 218 (2017).
[20] J. C. Johnston and V. Molinero, J. Am. Chem. Soc. **134**, 6650 (2012).
[21] M. A. Carignano, J. Phys. Chem. C **111**, 501 (2007).
[22] T. C. Hansen, M. M. Koza, and W. F. Kuhs, J. Phys.: Condens. Matter **20**, 285104 (2008).
[23] T. L. Malkin, B. J. Murray, A. V. Brukhno, J. Anwar, and C. G. Salzmann, Proc. Natl. Acad. Sci. U. S. A. **109**, 1041 (2012).
[24] E. B. Moore and V. Molinero, Phys. Chem. Chem. Phys. **13**, 20008 (2011).
[25] S. Choi, E. Jang, and J. S. Kim, J. Chem. Phys. **140**, 014701 (2014).
[26] M. Seo, E. Jang, K. Kim, S. Choi, and J. S. Kim, J. Chem. Phys. **137**, 154503 (2012).
[27] P. Pirzadeh and P. G. Kusalik, J. Am. Chem. Soc. **133**, 704 (2011).
[28] W. F. Kuhs, C. Sippel, A. Falenty, and T. C. Hansen, Proc. Natl. Acad. Sci. U. S. A. **109**, 21259 (2012).
[29] T. L. Malkin, B. J. Murray, C. G. Salzmann, V. Molinero, S. J. Pickering, and T. F. Whale, Phys. Chem. Chem. Phys. **17**, 60 (2015).
[30] B. J. Murray, T. L. Malkin, and C. G. Salzmann, J. Atmos. Sol.-Terr. Phys. **127**, 78 (2015).
[31] T. C. Hansen, M. M. Koza, P. Lindner, and W. F. Kuhs, J. Phys.: Condens. Matter **20**, 285105 (2008).
[32] B. J. Murray and A. K. Bertram, Phys. Chem. Chem. Phys. **8**, 186 (2006).
[33] K. Shimaoka, J. Phys. Soc. Jpn. **15**, 106 (1960).
[34] G. Honjo, N. Kitamura, K. Shimaoka, and K. Mihama, J. Phys. Soc. Jpn. **11**, 527 (1956).
[35] J. E. Shilling, M. A. Tolbert, O. B. Toon, E. J. Jensen, B. J. Murray, and A. K. Bertram, Geophys. Res. Lett. **33**, L17801, https://doi.org/10.1029/2006gl026671 (2006).
[36] F. V. Shallcross and G. B. Carpenter, J. Chem. Phys. **26**, 782 (1957).
[37] L. F. Keyser and M.-T. Leu, Microsc. Res. Tech. **25**, 434 (1993).
[38] G. Jancso, J. Pupezin, and W. A. Van Hook, J. Phys. Chem. **74**, 2984 (1970).
[39] K. Bielska, D. K. Havey, G. E. Scace, D. Lisak, A. H. Harvey, and J. T. Hodges, Geophys. Res. Lett. **40**, 6303, https://doi.org/10.1002/2013gl058474 (2013).
[40] V. Fernicola, L. Rosso, and M. Giovannini, Int. J. Thermophys. **33**, 1363 (2012).
[41] A. Wexler, J. Res. Natl. Bur. Stand., Sect. A **81**, 5 (1977).
[42] W. Wagner, A. Saul, and A. Pruss, J. Phys. Chem. Ref. Data **23**, 515 (1994).
[43] W. Wagner, T. Riethmann, R. Feistel, and A. H. Harvey, J. Phys. Chem. Ref. Data **40**, 043103 (2011).
[44] J. Marti and K. Mauersberger, Geophys. Res. Lett. **20**, 363, https://doi.org/10.1029/93gl00105 (1993).
[45] K. Mauersberger and D. Krankowsky, Geophys. Res. Lett. **30**, 1121, https://doi.org/10.1029/2002gl016183 (2003).
[46] G. F. Kraus and S. C. Greer, J. Phys. Chem. **88**, 4781 (1984).
[47] G. Beltramino, L. Rosso, D. Smorgon, and V. Fernicola, J. Chem. Thermodyn. **105**, 159 (2017).
[48] K. Scheel and W. Heuse, Ann. Phys. **334**, 723 (1909).
[49] G. Bottomley, Aust. J. Chem. **31**, 1177 (1978).
[50] P. Flubacher, A. J. Leadbetter, and J. A. Morrison, J. Chem. Phys. **33**, 1751 (1960).
[51] W. F. Giauque and J. W. Stout, J. Am. Chem. Soc. **58**, 1144 (1936).
[52] C. A. Angell, in *Water and Aqueous Solutions at Subzero Temperatures*, edited by F. Franks (Springer US, Boston, MA, 1982), p. 1.
[53] D. G. Archer and R. W. Carter, J. Phys. Chem. B **104**, 8563 (2000).
[54] E. Tombari, C. Ferrari, and G. Salvetti, Chem. Phys. Lett. **300**, 749 (1999).
[55] D. M. Murphy and T. Koop, Q. J. R. Meteorol. Soc. **131**, 1539 (2005).
[56] R. Feistel and W. Wagner, J. Phys. Chem. Ref. Data **35**, 1021 (2006).
[57] R. Feistel and W. Wagner, Geochim. Cosmochim. Acta **71**, 36 (2007).
[58] C. E. Bryson, V. Cazcarra, and L. L. Levenson, J. Chem. Eng. Data **19**, 107 (1974).
[59] N. J. Sack and R. A. Baragiola, Phys. Rev. B **48**, 9973 (1993).
[60] P. Löfgren, P. Ahlström, J. Lausma, B. Kasemo, and D. Chakarov, Langmuir **19**, 265 (2003).
[61] A. Kouchi, Nature **330**, 550 (1987).
[62] D. E. Brown, S. M. George, C. Huang, E. K. L. Wong, K. B. Rider, R. S. Smith, and B. D. Kay, J. Phys. Chem. **100**, 4988 (1996).
[63] R. S. Smith, J. Matthiesen, J. Knox, and B. D. Kay, J. Phys. Chem. A **115**, 5908 (2011).
[64] H. J. Fraser, M. P. Collings, M. R. S. McCoustra, and D. A. Williams, Mon. Not. R. Astron. Soc. **327**, 1165 (2001).
[65] S. La Spisa, M. Waldheim, J. Lintemoot, T. Thomas, J. Naff, and M. Robinson, J. Geophys. Res.: Planets **106**, 33351, https://doi.org/10.1029/2000je001305 (2001).
[66] O. Sneh, M. A. Cameron, and S. M. George, Surf. Sci. **364**, 61 (1996).
[67] P. M. Hundt, R. Bisson, and R. D. Beck, J. Chem. Phys. **137**, 074701 (2012).
[68] M. A. Tolbert and A. M. Middlebrook, J. Geophys. Res.: Atmos. **95**, 22423, https://doi.org/10.1029/jd095id13p22423 (1990).
[69] C. E. Bryson III, V. Cazcarra, and L. L. Levenson, J. Vac. Sci. Technol. **11**, 411 (1974).
[70] E. R. Batista, P. Ayotte, A. Bilić, B. D. Kay, and H. Jónsson, Phys. Rev. Lett. **95**, 223201 (2005).
[71] K. D. Gibson, D. R. Killelea, H. Yuan, J. S. Becker, and S. J. Sibener, J. Chem. Phys. **134**, 034703 (2011).
[72] M. A. Floriano, Y. P. Handa, D. D. Klug, and E. Whalley, J. Chem. Phys. **91**, 7187 (1989).
[73] Y. P. Handa, O. Mishima, and E. Whalley, J. Chem. Phys. **84**, 2766 (1986).
[74] A. Hallbrucker and E. Mayer, J. Phys. Chem. **91**, 503 (1987).
[75] J. A. Ghormley, J. Chem. Phys. **48**, 503 (1968).
[76] A. Hallbrucker, E. Mayer, and G. P. Johari, J. Phys. Chem. **93**, 4986 (1989).
[77] D. R. MacFarlane and C. A. Angell, J. Phys. Chem. **88**, 759 (1984).

[78]Y. P. Handa, D. D. Klug, and E. Whalley, J. Chem. Phys. **84**, 7009 (1986).
[79]J. A. McMillan and S. C. Los, Nature **206**, 806 (1965).
[80]M. Sugisaki, H. Suga, and S. Seki, Bull. Chem. Soc. Jpn. **41**, 2591 (1968).
[81]E. Mayer and A. Hallbrucker, Nature **325**, 601 (1987).
[82]T. Hondoh, T. Itoh, S. Amakai, K. Goto, and A. Higashi, J. Phys. Chem. **87**, 4040 (1983).
[83]F. Smallenburg, P. H. Poole, and F. Sciortino, Mol. Phys. **113**, 2791 (2015).
[84]A. Zaragoza, M. M. Conde, J. R. Espinosa, C. Valeriani, C. Vega, and E. Sanz, J. Chem. Phys. **143**, 134504 (2015).
[85]D. Quigley, J. Chem. Phys. **141**, 121101 (2014).
[86]E. H. G. Backus and M. Bonn, J. Chem. Phys. **121**, 1038 (2004).
[87]T. Kondo, H. S. Kato, M. Bonn, and M. Kawai, J. Chem. Phys. **126**, 181103 (2007).
[88]P. Jenniskens and D. F. Blake, Astrophys. J. **473**, 1104 (1996).
[89]M. Kumai, J. Glaciol. **7**, 95 (1968).
[90]L. G. Dowell and A. P. Rinfret, Nature **188**, 1144 (1960).
[91]W. F. Kuhs, D. V. Bliss, and J. L. Finney, J. Phys. Colloques **48**, C1 (1987).
[92]G. P. Arnold, E. D. Finch, S. W. Rabideau, and R. G. Wenzel, J. Chem. Phys. **49**, 4365 (1968).
[93]H. Tanaka and I. Okabe, Chem. Phys. Lett. **259**, 593 (1996).
[94]H. Tanaka, J. Chem. Phys. **108**, 4887 (1998).
[95]D. W. Fahey, R. S. Gao, O. Möhler, H. Saathoff, C. Schiller, V. Ebert, M. Krämer, T. Peter, N. Amarouche, L. M. Avallone, R. Bauer, Z. Bozóki, L. E. Christensen, S. M. Davis, G. Durry, C. Dyroff, R. L. Herman, S. Hunsmann, S. M. Khaykin, P. Mackrodt, J. Meyer, J. B. Smith, N. Spelten, R. F. Troy, H. Vömel, S. Wagner, and F. G. Wienhold, Atmos. Meas. Tech. **7**, 3177 (2014).
[96]E. Mayer and R. Pletzer, Nature **319**, 298 (1986).
[97]G. A. Kimmel, K. P. Stevenson, Z. Dohnalek, R. S. Smith, and B. D. Kay, J. Chem. Phys. **114**, 5284 (2001).
[98]G. A. Kimmel, Z. Dohnálek, K. P. Stevenson, R. S. Smith, and B. D. Kay, J. Chem. Phys. **114**, 5295 (2001).
[99]Z. Dohnalek, G. A. Kimmel, P. Ayotte, R. S. Smith, and B. D. Kay, J. Chem. Phys. **118**, 364 (2003).
[100]C. R. Hill, C. Mitterdorfer, T. G. A. Youngs, D. T. Bowron, H. J. Fraser, and T. Loerting, Phys. Rev. Lett. **116**, 215501 (2016).
[101]U. Raut, M. Fama, B. D. Teolis, and R. A. Baragiola, J. Chem. Phys. **127**, 204713 (2007).
[102]K. P. Stevenson, G. A. Kimmel, Z. Dohnalek, R. S. Smith, and B. D. Kay, Science **283**, 1505 (1999).
[103]C. Mitterdorfer, M. Bauer, T. G. A. Youngs, D. T. Bowron, C. R. Hill, H. J. Fraser, J. L. Finney, and T. Loerting, Phys. Chem. Chem. Phys. **16**, 16013 (2014).
[104]A. Kouchi, T. Yamamoto, T. Kozasa, T. Kuroda, and J. M. Greenberg, Astron. Astrophys. **290**, 1009 (1994).
[105]A. Sepúlveda, E. Leon-Gutierrez, M. Gonzalez-Silveira, C. Rodríguez-Tinoco, M. T. Clavaguera-Mora, and J. Rodríguez-Viejo, J. Chem. Phys. **137**, 244506 (2012).
[106]R. J. Speedy, J. Phys. Chem. **91**, 3354 (1987).
[107]E. H. Mitchell, U. Raut, B. D. Teolis, and R. A. Baragiola, Icarus **285**, 291 (2017).
[108]R. Scott Smith, C. Huang, E. K. L. Wong, and B. D. Kay, Surf. Sci. **367**, L13 (1996).
[109]W. Hage, A. Hallbrucker, E. Mayer, and G. P. Johari, J. Chem. Phys. **103**, 545 (1995).
[110]S. D. Guzewich, E. R. Talaat, A. D. Toigo, D. W. Waugh, and T. H. McConnochie, J. Geophys. Res.: Planets **118**, 1177, https://doi.org/10.1002/jgre.20076 (2013).
[111]M. Vincendon, C. Pilorget, B. Gondet, S. Murchie, and J. P. Bibring, J. Geophys. Res.: Planets **116**, E00j02, https://doi.org/10.1029/2011je003827 (2011).
[112]L. Maltagliati, F. Montmessin, A. Fedorova, O. Korablev, F. Forget, and J. L. Bertaux, Science **333**, 1868 (2011).
[113]E. J. Jensen, J. B. Smith, L. Pfister, J. V. Pittman, E. M. Weinstock, D. S. Sayres, R. L. Herman, R. F. Troy, K. Rosenlof, T. L. Thompson, A. M. Fridlind, P. K. Hudson, D. J. Cziczo, A. J. Heymsfield, C. Schmitt, and J. C. Wilson, Atmos. Chem. Phys. **5**, 851 (2005).
[114]T. Peter, C. Marcolli, P. Spichtinger, T. Corti, M. B. Baker, and T. Koop, Science **314**, 1399 (2006).